Journal of Biomechanics 47 (2014) 1368–1372

Contents lists available at ScienceDirect

Journal of Biomechanics

journal homepage: www.elsevier.com/locate/jbiomech
www.JBiomech.com

Identification of rheological properties of human body surface tissue

Vincas Benevicius, Rimvydas Gaidys, Vytautas Ostasevicius *, Vaidotas Marozas

Kaunas University of Technology, Studentų g. 65, 51369 Kaunas, Lithuania

ARTICLE INFO

Article history:
Accepted 31 January 2014

Keywords:
Motion analysis
Soft tissue artifact
Mathematical model
Tissue rheology
Body mass index

ABSTRACT

According to World Health Organization obesity is one of the greatest public health challenges of the 21st century. It has tripled since the 1980s and the numbers of those affected continue to rise at an alarming rate, especially among children. There are number of devices that act as a prevention measure to boost person's motivation for physical activity and its levels. The placement of these devices is not restricted thus the measurement errors that appear because of the body rheology, clothes, etc. cannot be eliminated. The main objective of this work is to introduce a tool that can be applied directly to process measured accelerations so human body surface tissue induced errors can be reduced. Both the modeling and experimental techniques are proposed to identify body tissue rheological properties and prelate them to body mass index. Multi-level computational model composed from measurement device model and human body surface tissue rheological model is developed. Human body surface tissue induced inaccuracies can increase the magnitude of measured accelerations up to 34% when accelerations of the magnitude of up to 27 m/s^2 are measured. Although the timeframe of those disruptions are short – up to 0.2 s – they still result in increased overall measurement error.

1. Introduction

The placement of devices that act as prevention measure to boost persons motivation for physical activity, is not restricted thus the errors can skew the output of the measurement system. These errors fall into categories on instrumental and errors of soft tissue artifacts (Chiari et al., 2005; Lucchetti et al., 1998). Soft tissue artifact is defined as an error that originates at the interface between the measurement instrument and the substrate which is the object of the measurement (Cappozzo et al.,1996).

Soft tissue artifact is believed to be the largest invalidating source of experimental error (Stagni et al., 2003; Cappello et al., 1997). Unfortunately, this error is also the most difficult to eliminate due to several factors, including it being subject and task dependent. The overall goal of the work by Manal et al. (2000) is to determine an optimal surface-tracking marker set for tracking motion of the tibia during natural cadence walking. The work of Bergstrom and Boyce (2001) dicusses a new constitutive model capable of capturing the experimentally observed behavior under different general multiaxial loading conditions. A fully variational costitutive model of soft biological tissues is formulated in paper by El Sayed et al. (2008). A simple method for constructing transversely isotropic polyconvex functions suitable for the description of biological soft tissues is provided in the work of Balzani et al. (2006). Soft tissue compartment vibrations are initiated at heel-strike in heel-toe running (Boyer and Nigg, 2007). The relationship between measured displacement and stiffness in gel and tissue in vitro is presented by Konofagou et al. (2004). To determine the strain and stress in the biological soft tissues the anisotropic hyperelastic costitutive laws are used by Peyraut et al. (2009) in the context of finite element and analytical analysis. By using a non-invasive approach, Gao and Zheng (2008) investigated the soft tissue movement on the thigh and shank of 20 healthy subjects during level walking which is one of the most important human daily activities and the basic content of clinical gait analysis.

With miniaturization and broad spread of MEMS systems like accelerometers in end user devices more and more applications emerge. However these devices are prone to soft tissue artifacts for one simple reason: they are always worn mounted somewhere on the body surface. While instrumental errors can be reduced with higher quality and precision hardware, soft tissue artifacts are still left aside although soft tissue artifacts usually are of greater magnitude compared to instrumental errors. For this reason this research work is proposed.

2. Human body surface tissue rheological model and its validation

The chest area (Fig. 1) was chosen to form the multi-level computational model that consists of two different parts:

* Corresponding author. Tel.: +370 698 12588.
E-mail address: vytautas.ostasevicius@ktu.lt (V. Ostasevicius).

http://dx.doi.org/10.1016/j.jbiomech.2014.01.050
0021-9290

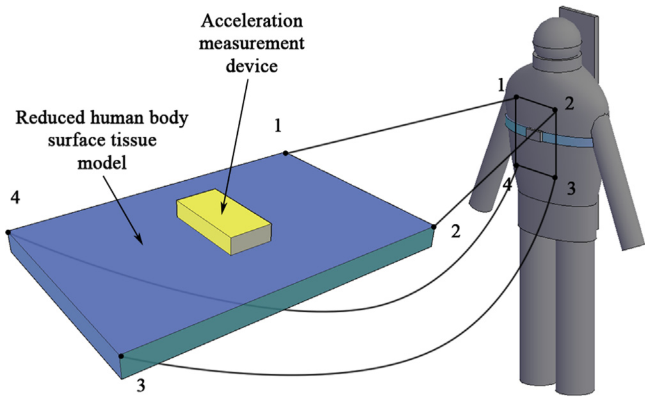

Fig. 1. Model scheme showing its location and parts.

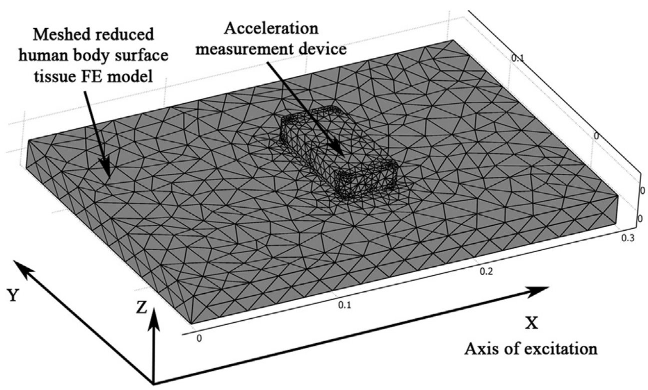

Fig. 2. Meshed FE model in the COMSOL with excitation axis presented.

an acceleration measurement device model and human body surface tissue rheological model.

Geometrical size of acceleration measurement device is $80 \times 40 \times 16$ mm, mass 42 g. Its density can be said to be 806 kg/m^3.

Initial pre-stress is described as

$$\mathbf{Ku} = \mathbf{F} \tag{1}$$

where $\mathbf{K}$ is the stiffness matrix, $\mathbf{u}$ is the displacement vector and $\mathbf{F}$ is the force vector.

Human body surface tissue rheological model (Fig. 2) is selected to be hyper elastic Neo-Hookean material. Its geometrical size $300 \times 200 \times 20$ mm. Given size completely covers the area where the acceleration measurement device movement mismatch exists. Initial shear modulus is chosen to be 100 Pa (Markidou et al., 2005), initial bulk modulus 0.1 GPa (Gennisson et al., 2004; Mukherjee et al., 2005), density was set to 1000 kg/m^3.

In the given finite elements COMSOL formulation the dynamics of the human body model is described by the following equation of motion by taking into account that base motion law is known

$$\begin{bmatrix} \mathbf{M}_{NN} & \mathbf{M}_{NK} \\ \mathbf{M}_{KN} & \mathbf{M}_{KK} \end{bmatrix} \begin{Bmatrix} \ddot{\mathbf{u}}_N \\ \ddot{\mathbf{u}}_K \end{Bmatrix} + \begin{bmatrix} \mathbf{C}_{NN} & \mathbf{C}_{NK} \\ \mathbf{C}_{KN} & \mathbf{C}_{KK} \end{bmatrix} \begin{Bmatrix} \dot{\mathbf{u}}_N \\ \dot{\mathbf{u}}_K \end{Bmatrix} + \begin{bmatrix} \mathbf{K}_{NN} & \mathbf{K}_{NK} \\ \mathbf{K}_{KN} & \mathbf{K}_{KK} \end{bmatrix} \begin{Bmatrix} \mathbf{u}_N \\ \mathbf{u}_K \end{Bmatrix} = \begin{Bmatrix} \mathbf{0} \\ \mathbf{r} \end{Bmatrix} \tag{2}$$

where nodal displacement vectors $\mathbf{u}_N(t)$ and $\mathbf{u}_K(t)$ correspond to displacement of free nodes and kinematically excited nodes respectively; $\mathbf{M}$, $\mathbf{C}$ and $\mathbf{K}$ are the mass, damping and stiffness matrices respectively; $\mathbf{r}$ is a vector representing reaction forces of the kinematically excited nodes.

Displacement vector of unconstrained nodes is expressed as

$$\mathbf{u}_N = \mathbf{u}_{Nrel} + \mathbf{u}_{Nk} \tag{3}$$

where $\mathbf{u}_{Nrel}$ denotes a component of relative displacement with respect to moving base displacement $\mathbf{u}_{Nk}$.

Vectors $\mathbf{u}_{Nk}$ and $\mathbf{u}_K$ correspond to rigid-body displacements which do not induce internal elastic forces in the structure. Proportional damping approach is adopted in the form

$$\mathbf{C} = \alpha\mathbf{M} + \beta\mathbf{K} \tag{4}$$

with α and β are the Rayleigh damping constants.

Hence, the following matrix equation is obtained after the algebraic rearrangements of previous equations and contains matrices of the structure constrained in the nodes of imposed kinematic excitation

$$\mathbf{M}_{NN}\ddot{\mathbf{u}}_{Nrel} + \mathbf{C}_{NN}\dot{\mathbf{u}}_{Nrel} + \mathbf{K}_{NN}\mathbf{u}_{Nrel} = \widehat{\mathbf{M}} \tag{5}$$

here $\widehat{\mathbf{M}}$ represents a vector of inertial forces that act on each node of the structure as a result of applied kinematic excitation and is expressed as

$$\widehat{\mathbf{M}} = \mathbf{M}_{NN}\mathbf{K}_{NN}^{-1}\mathbf{K}_{NK} - \mathbf{M}_{NK}. \tag{6}$$

Model validation was performed by utilizing experimental vertical jump data (Benevicius et al., 2013). To compare the output of the model with experimental data three curves were plotted (Fig. 3).

As can be seen in Fig. 3 modeling results fit the experimental data. Average error was defined as

$$e = \frac{\sum_{i=1}^{N} |y_i - \widehat{y}_i|}{N} \tag{7}$$

where y_i is the experimental data point; $\widehat{y}_i$ is the modeled data point; N is the number of data points.

For the experimental data set average error was 0.0034, maximum error 0.0136. This means that the average difference between experimental data point and model output data point was 0.0034 m (3.4 mm). Average jump height was 154.3 mm. If this average is taken as a base, it can be said that model has average relative error of 2.2%. Maximum relative error was lower than 8.9%. It can be concluded that the model corresponds well to the real world object.

3. Human body surface tissue rheological model analysis

Validated tissue rheological model is further analyzed to get deeper insight in its behavior. Axes of reference used during the analysis are given in Fig. 2. Axis X corresponds to the vertical body movement.

Fig. 4 shows how the displacement on the skin surface is different through the area reaching its maximum just under the attached device. During jump whole soft tissue is moving differently from underlying bones, attached device impacts surrounding

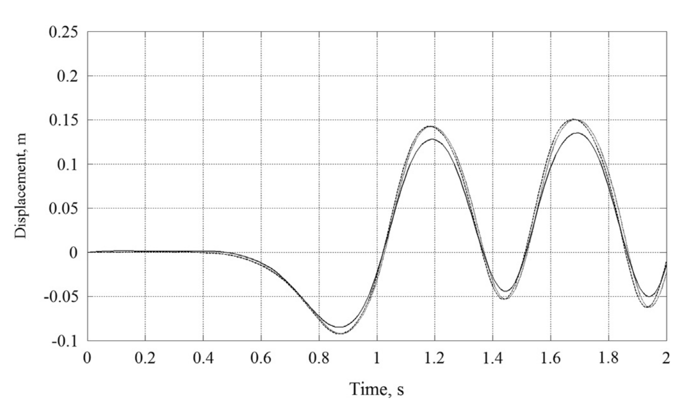

Fig. 3. Experimental vertical jump data when no surface tissue impact is present (solid line); acceleration measurement device movement during experiment (dotted line); modeled acceleration measurement device movement (dashed line).